FINITE ELEMENT ANALYSIS OF DISPERSION IN WAVEGUIDES WITH SHARP METAL EDGES

J. P. Webb

Computational Analysis and Design Laboratory
Department of Electrical Engineering, McGill University
3480 University St., Montreal, H3A 2A7, Canada

ABSTRACT

The dispersion characteristics of arbitrarily-shaped waveguides with sharp metal edges are found by a finite element method in which the usual polynomials are supplemented by singular trial functions. As in recent approaches, the method solves for the three components of magnetic field and can thereby avoid spurious modes.

INTRODUCTION

Waveguides with sharp metal edges are widely used at microwave frequencies: examples are ridge guide, microstrip, slot-line and fin-line. It is often necessary to be able to predict dispersion in such waveguides and numerous analytical techniques have been developed for particular geometries. For example, the singular integral equation [1] and spectral domain methods [2] have been used to find dispersion curves for planar waveguides with infinitely-thin conductors. Of the techniques capable of analysing arbitrary geometries, there has been some success with finite element and finite difference methods which use two axial field components as unknowns. However this approach cannot handle generally-anisotropic materials and, more seriously, suffers from the presence of spurious solutions. For these reasons, a better approach is to use the three-component magnetic field, **H**, as the unknown [3]. The finite element method in this case finds the stationary points of the following functional:

$$F(\mathbf{H}) = \int_S \Big[(\nabla\times\mathbf{H})^* \cdot \epsilon_r^{-1} \cdot (\nabla\times\mathbf{H}) + s\,|\nabla\cdot\mu_r\mathbf{H}|^2 - k_o^2\,\mathbf{H}^*\cdot\mu_r\cdot\mathbf{H}\Big]\,dS \qquad (1)$$

$*$ denotes complex-conjugate; S is the cross-section of the waveguide; ϵ_r and μ_r are the relative permittivity and permeability tensors. The variation of **H** with time and with the axial coordinate z is of the form $\exp(j\omega t - j\beta z)$, where ω is the angular frequency (rads/s) and β is the phase constant (rads/m). k_o is the wavenumber, ω/c, where c is the velocity of light in vacuo. The term involving the divergence of **H** is a penalty term [3], added to remove spurious modes. s is a real scalar, called the penalty parameter. The stationary points $(\mathbf{H}, k_o)$ of F are the modes of the waveguide which have the specified value of β. A similar functional exists for the electric field.

Unfortunately, the transverse part of the magnetic or electric field is infinite at a sharp edge of a perfectly-conducting boundary [4]. This is quite different to the behaviour of the axial components, or of the potential used in quasi-static analysis - these variables have infinite derivatives at such an edge, but are themselves finite. The three-component methods presented to date do not adequately address the problems that this singularity poses. The methods have used as basis functions the piecewise-polynomials traditionally associated with finite elements. It is clear that such trial functions cannot represent accurately an infinite field.

SINGULAR TRIAL FUNCTIONS

A solution to this problem is to supplement the polynomials with singular trial functions, a technique that has been often used for dependent variables which have infinite derivatives. A typical sharp edge, and cylindrical coordinates based on it, are shown in Figure 1.

Let α be the interior angle at the edge, in radians between π and 2π. The transverse magnetic field near a sharp edge, when no magnetic material is present, is the gradient of a harmonic function which satisfies Neumann boundary conditions on the two conducting surfaces [4]. Starting from this, the field may be expressed as a series in powers of r, of which just the first m_o terms are singular:

0149-645X/88/0000-0391$01.00 © 1988 IEEE

$$H_t = \sum_{m=1}^{m_o} A_m \mathbf{f}_m(r, \varphi) + O(r) \qquad (2)$$

where A_m are arbitrary coefficients and

$$\mathbf{f}_m = r^{mq-1}\left[\mathbf{a}_r \cos(mq(\varphi-\varphi_o)) - \mathbf{a}_\varphi \sin(mq(\varphi-\varphi_o))\right] \qquad (3)$$

$$q = \frac{\pi}{\alpha} \qquad \text{and} \qquad m_o = \mathrm{int}\left[\frac{2}{q}\right]$$

$\mathbf{a}_r$ and $\mathbf{a}_\varphi$ are unit vectors in the radial and azimuthal directions respectively. There are a maximum of three singular functions $\mathbf{f}_m$ for each sharp edge. Of these, only the first is infinite at the edge; the remainder have infinite derivatives. A similar expansion is possible for the transverse electric field.

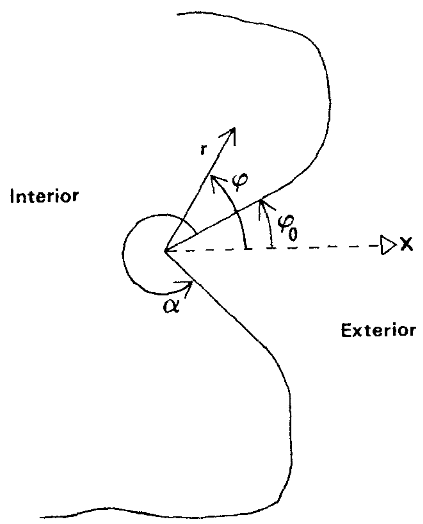

Figure 1: The cylindrical coordinate system based on a sharp edge of a perfectly-conducting boundary.

Suppose that for the problem as a whole, there are M such singular functions, $\mathbf{f}_1, \ldots, \mathbf{f}_M$. One trial function $\mathbf{g}_m$ may defined for each of these, such that in any triangle:

$$\mathbf{g}_m(\mathbf{r}) = \mathbf{f}_m(\mathbf{r}) - \sum_{n=1}^{n_o} \mathbf{f}_{mn}\alpha_n(\mathbf{r}) \qquad (4)$$

Here $\mathbf{r}$ is the position vector; α_n are the usual n_o Lagrange polynomials associated with triangular finite elements [5]; and $\mathbf{f}_{mn}$ is the value of $\mathbf{f}_m$ at the nth node of the triangle, or zero if $\mathbf{f}_m$ is infinite at the nth node. The functions $\mathbf{g}_m$ are so constructed that they have the same behaviour as the corresponding $\mathbf{f}_m$ near the latter's singular point, but they vanish at every other node of the finite element mesh.

The magnetic field in any triangle then takes the form:

$$\mathbf{H}(\mathbf{r}) = \sum_{n=1}^{n_o} \mathbf{H}_n\alpha_n(\mathbf{r}) + \sum_{m=1}^{M} K_m\mathbf{g}_m(\mathbf{r}) \qquad (5)$$

where $\mathbf{H}_n$ are the unknown values of magnetic field at n_o nodes of the triangle; and K_m are the unknown coefficients of the singular trial functions.

To evaluate the functional F (1) for a magnetic field of the form (5), a certain amount of integration must be performed. Those integrals which do not involve the singular trial functions were carried out in closed form by making use of the concept of the universal matrix [5]; for the remainder, Gaussian integration was used. Finally, the stationary points of the functional F are given by the eigensolutions of the matrix equation:

$$(\mathbf{A} + s\mathbf{C})\ \mathbf{x} = k_o^2\ \mathbf{B}\ \mathbf{x} \qquad (6)$$

where **A**, **B** and **C** are large, sparse, square, Hermitian matrices, and $\mathbf{x}$ is a column vector whose entries are the unknown components of magnetic field at the nodes, and the coefficients K_m. Efficient methods exist for finding the first few eigenvalues and corresponding eigenvectors of this sparse matrix equation; in the present instance, the Trace Minimization method is used [6]. This method requires the storage and manipulation of only the nonzero entries of the matrices, and has a complexity which is roughly $O(N^2)$, where N is the matrix dimension. A modification of the algorithm [7] allows for the automatic adjustment of the penalty parameter s during solution, to eliminate spurious modes. However, when just the slow-wave region is of interest, it is sufficient to hold the penalty parameter fixed at 1.0 [8], and this approach was taken for the microstrip problems below.

RESULTS

Figure 2 shows a rectangular waveguide with twin double ridges. This structure is air-filled and has modes which are TE or TM, so it could be more efficiently analyzed with a single longitudinal component of **E** or H. However, it was chosen as a test problem because it has 8 sharp edges (4 in the half problem).

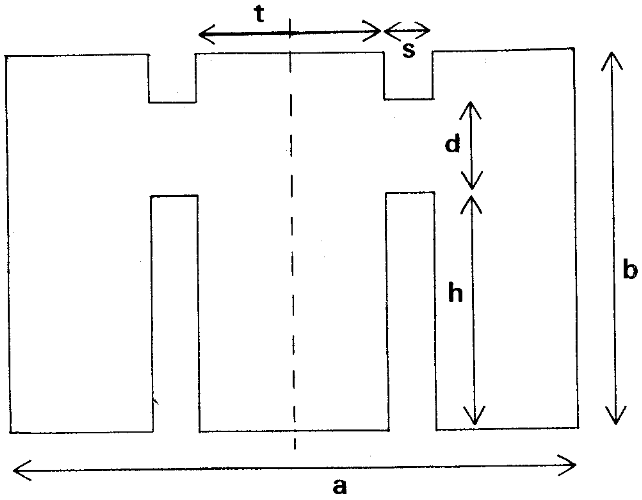

Figure 2: Rectangular waveguide with two double ridges. b/a=0.5, d/b=0.1, s/a=0.125, h/b=0.7, t/a=0.5. The broken line is a plane of symmetry.

One half of the problem was analyzed, using 42 second-order elements and 8 singular trial functions. To get the two lowest modes, it was necessary to solve two problems: one with an electric wall and with a magnetic wall on the plane of symmetry. Each problem was analyzed twice, once with the magnetic field as the unknown and once with the electric field. Since the lowest two modes are TE, the magnetic field was entirely axial, and did not involve the singular trial functions; the electric field is of more interest, because it is transverse and infinite at the sharp edges. The cut-off frequencies have been previously obtained with an accuracy of about 1% [9]. See Table 1.

Mode	FE Solution		Ref. [9]
	Magnetic	Electric	
Dominant	0.923	0.904	0.911
Subdominant	1.177	1.150	1.161

Table 1: The cut-off wave-number, k_o (rads/m), for the first two modes of the waveguide shown in Figure 2.

The electric field cases were also solved without singular trial functions, but with the field constrained to be in the direction of an average normal at each sharp edge. The first two wave-numbers were extremely inaccurate: 3.05 rads/m and 3.23 rads/m respectively.

A second test problem was the shielded microstrip shown in Figure 3. One half of the problem was analysed, with a magnetic wall on the plane of symmetry. 73 second-order elements were used (most of them placed close to the central conducting strip). The dispersion curves for the lowest two modes are shown in Figure 4, for an isotropic dielectric.

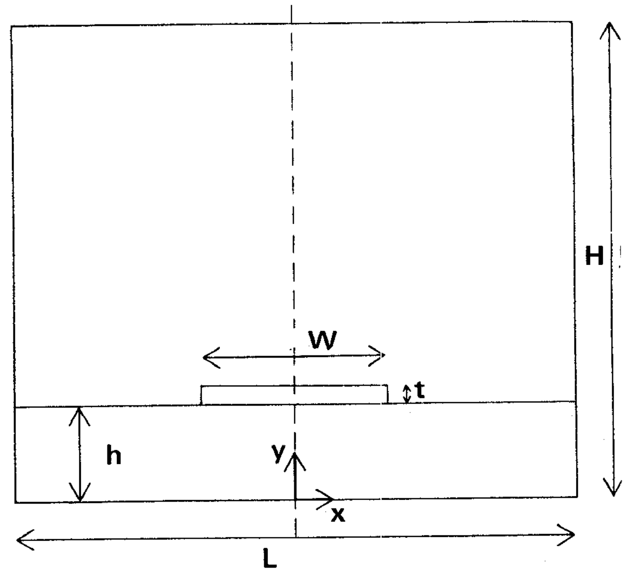

Figure 3: A shielded microstrip transmission line. The broken line shows the plane of symmetry. L=12.7mm, W=1.27mm, h=1.27mm, H=12.7mm.

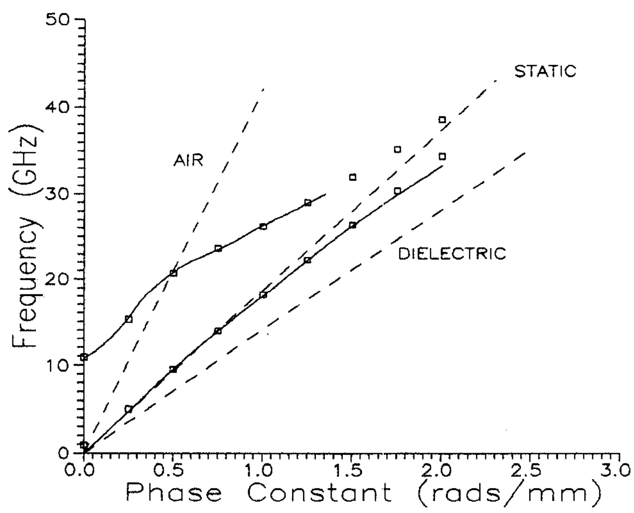

Figure 4: Dispersion curves for the first two modes of the transmission line of Figure 3, with a magnetic wall at the plane of symmetry. Isotropic substrate, ϵ_r=8.875, t=0. The solid line for the lowest mode is from [1]; the solid line for the next mode is from [10]; squares are finite-element results. The broken line marked STATIC is the low-frequency approximation for the dominant mode, from Wheeler [11].

The same microstrip was then solved with an anisotropic substrate. The results are shown in Figure 5.

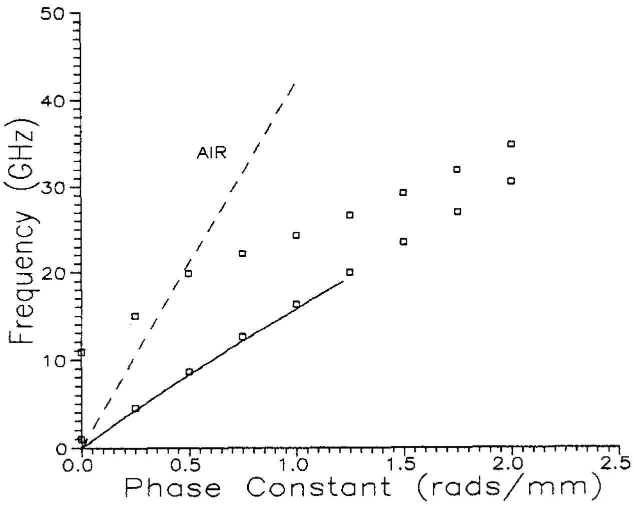

Figure 5: Dispersion curves for the first two modes of the transmission line of Figure 3, with a magnetic wall at the plane of symmetry. Saphire substrate: $\epsilon_{rxx}=9.4$, $\epsilon_{ryy}=11.6$ and $\epsilon_{rzz}=9.4$. $t=0$. The solid line is from [12], with no shield present.

A thick strip was also analysed ($t/h = 0.05$). The transverse part of the magnetic field is shown in Figure 6.

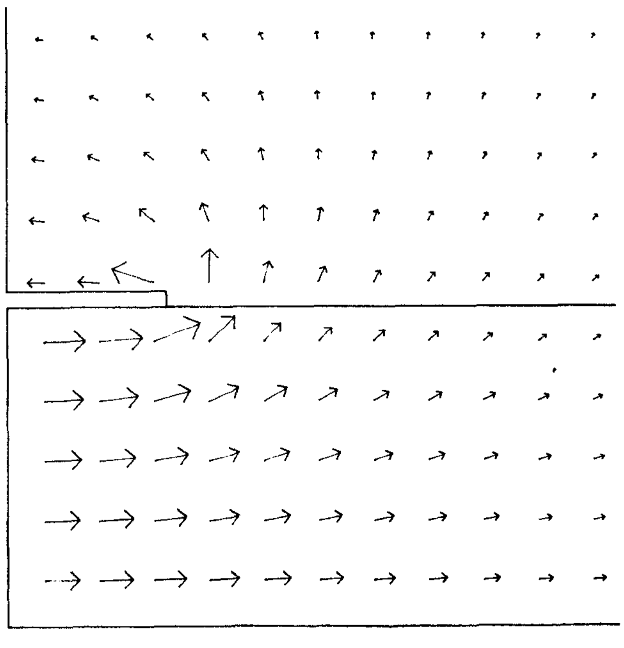

Figure 6: Transverse part of the magnetic field, in the vicinity of the strip, for the transmission line of Figure 3. $\epsilon_r=8.875$, $t/h = 0.05$. The left-hand edge of the diagrams corresponds to the plane of symmetry in Figure 3. The frequency is 11.3 GHz.

ACKNOWLEDGEMENTS

I would like to thank the Natural Sciences and Engineering Council of Canada for financial support for this work.

REFERENCES

[1] Mittra, R., Itoh, T., 'A new technique for the analysis of the dispersion characteristics of microstrip line', IEEE Trans., MTT-19, no. 1, pp. 47-56, January 1971.
[2] Itoh, T., Mittra, R., 'Spectral-domain approach for calculating the dispersion characteristcs of microstrip lines', IEEE Trans., MTT-21, pp. 496-499, July, 1973.
[3] Rahman, B. M. A., Davies, J. B., 'Finite element analysis of optical and microwave problems', IEEE Trans., MTT-32, no. 1, pp. 20-28, January, 1984.
[4] Van Bladel, J., 'Field singularities at metal-dielectric wedges', IEEE Trans., AP-33, no. 4, pp. 450-455, April, 1985.
[5] Silvester, P., Ferrari, R. L., 'Finite elements for electrical engineers', Cambridge University Press, 1983.
[6] Sameh, A. H., Wisniewski, J. A., 'A trace minimization algorithm for the generalized eigenvalue problem', SIAM J. Numer. Anal., vol. 19, no. 6, pp. 1243-1259, Dec. 1982.
[7] Webb, J. P., 'Efficient generation of divergence-free fields for the finite element analysis of 3D cavity resonances', COMPUMAG 1987, Graz, Austria; to appear in IEEE Trans. on Magnetics.
[8] Koshiba, M., Hayata, K., Suzuki, M., 'Improved finite-element formulation in terms of the magnetic vector for dielectric waveguides', IEEE Trans., MTT-33, no. 3, pp. 227-233, March, 1985.
[9] Dasgupta, D., Saha, P. K., 'Rectangular waveguide with two double ridges', IEEE Trans., MTT-31, no. 11, pp. 938-941, November, 1983.
[10] Mirshekar-Syahkal, D., Davies, J. B., 'Accurate solution of microstrip and coplanar structures for dispersion and for dielectric and conductor losses', IEEE Trans., MTT-27, no. 7, pp. 694-699, July, 1979.
[11] Wheeler, H. A., 'Transmission-line properties of a strip on a dielectric sheet on a plane', IEEE Trans., MTT-25, no. 8, pp. 631-643, August, 1977.
[12] Kretch, B. E., Collin, R. E., 'Microstrip dispersion including anisotropic substrates', IEEE Trans., MTT-35, no. 8, pp. 710-718, August, 1987.